 doi.org/10.52568/001625/JCSP/47.01.2025

Synthesis, Photoelectrochemical and Aggregation Properties of Two New 8-hydroxyquinoline Derivatives

Xueling Zheng

School of Health Caring Industry, Shandong Institute of Commerce and Technology, Jinan 250103, Shandong, China.

zhengxueling2023@outlook.com*

(Received on 28th August 2023, accepted in revised form 23rd August 2024)

Summary: Two new 8-hydroxyquinoline (8-HQ) derivatives, namely 5-((4-chlorobenzene) diazene) -8-hydroxyquinoline (N-HQ) and 5-((4-chlorobenzene) methylene amino) -8-hydroxyquinoline (C-HQ), were designed and synthesized. Their structures were characterized by ^{1}H NMR, ^{13}C NMR, FT-IR and HR-MS. Their physical and photoelectrochemical properties were studied by absorption, emission, electrochemistry and thermog ravimetry. In addition, the gaussian program was used to calculate the geometric configurations of the two derivatives. Since N-HQ has an approximate planar configuration, it is packed in a highly ordered molecule packing in the solid state. However, there is a transverse offset between adjacent C-HQ molecules. The results show that the subtle difference of molecular structure can have a great influence on the properties of 8-HQ derivatives. This study also explored the application potential of C-HQ in fluorine ion fluorescence detection.

Key words: 8-hydroxyquinoline, Synthesis, Absorption, Emission, Aggregation

Introduction

8-Hydroxyquinoline (8-HQ) derivatives are crucial molecules in the fields of molecular recognition, biochemistry, drug synthesis, preparation of organic luminescent materials, light-emitting devices, and corrosion inhibitors [1-3]. These derivatives play various roles due to their chelating ability, high fluorescence efficiency, good film forming, simple purification and excellent thermal stability [4-7]. By studying its luminescence mechanism, research has shown that the luminescence color, luminescence intensity, and other properties of 8-HQ itself and its metal complexes can be adjusted by connecting different substituent groups to 8-HQ [8-11]. Given that hydroxyl is a strong ortho-para-positioning group, derivations of 8-HQ often occur at the ortho-para-positions of hydroxyl (8-HQ positions 5 and 7) [12-16]. Therefore, connecting different substituent groups at the fifth position is a key strategy for regulating the properties of 8-HQ derivatives [17-20]. E. Ahmetali prepared unsymmetrical zinc(II) phthalocyanine derivatives bearing one 8-HQ group and three tert-butyl groups (8-MeQ-ZnPc and 8-HQ-ZnPc). The fluorescence, singlet oxygen, and photodegradation quantum yields indicate that these photosensitizers are promising anticancer agent candidates [21]. P. Mei synthesized three 8-HQ derivatives: 12N-HQ, 12O-HQ, and 12S-HQ by introducing different substituents at position 5. The potentiodynamic polarization results demonstrated that all three compounds acted as mixed corrosion inhibitors [22].

In this work, two new 8-HQ derivatives with extended π system, 5-((4- chlorobenzene) diazene) -8-hydroxyquinoline (N-HQ) and 5-((4-chlorobenzene) methylene amino) -8-hydroxyquinoline (C-HQ) (Scheme 1), were designed and synthesized. The synthesis involved the Reimer-Tiemann reaction, Schiff base synthesis reaction, and diazotization reaction, which connected phenyl groups to the 5-position of 8-HQ via C=N bond and N=N bond, respectively. These derivatives were fully characterized by ^{1}H NMR, ^{13}C NMR, FT-IR and HR-MS. Additionally, various photochemical properties and aggregation behaviors of the two derivatives were thoroughly investigated, and theoretical calculations were conducted to reveal the effect of structural differences on their properties. The application potential of C-HQ in fluorine ion (F^-) fluorescence detection was also explored.

*To whom all correspondence should be addressed.

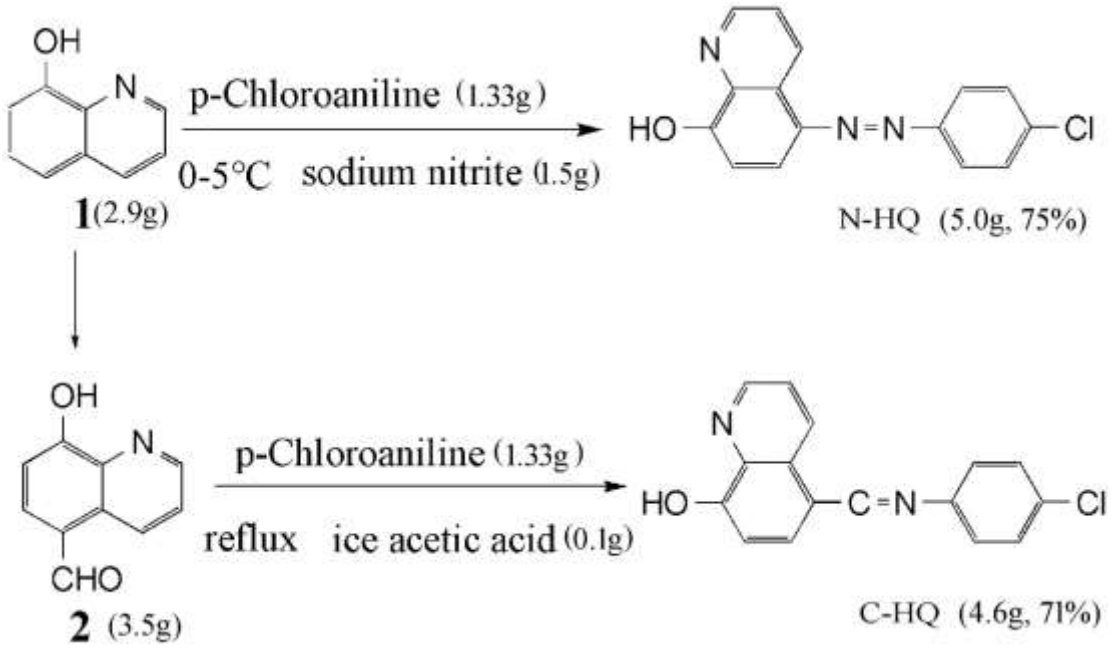

Scheme-1: The synthetic route of N-HQ and C-HQ.

Experimental

Materials and instrumental methods

All chemicals and solvents were purchased from commercial source, and were reagent grade for direct use without further purification. ^{1}H NMR and ^{13}C NMR spectra were recorded in $CDCl_3$ with a Bruker Advance 300 spectrometer at room temperature. FT-IR spectra were recorded on the Bruker Tensor-27 spectrophotometer. Mass spectra were measured using a Bruker Maxis UHR-TOF MS spectrometer. UV−Vis absorption spectra were recorded using a Varian CARY-50 spectrophotometer. Fluorescence spectra were recorded using a Hitachi FL-4500 spectrofluorometer. Electrochemistry testing was conducted using a CH 1604C electrochemical analyzer with platinum wire, $Ag/AgNO_3$ (Ag/Ag^+), and glassy carbon (diameter: 1.6 mm; area 0.02 cm^2) as counter electrode, reference electrode, and working electrode, respectively. Tetrabutylammonium hexafluorophosphate ($TBAPF_6$) was used as an electrolyte to calibrate the external potential according to the ferrocene/ferrocenium couple. Thermogravimetric analysis (TGA) was performed using a TA Q50 instrument, and the sample temperature was maintained at 10 ℃/ min in a N_2 atmosphere. Scanning electron microscopic (SEM) measurements were performed with a FEI NOVA NANOSEM 450 microscope. Powder X-ray diffraction (XRD) patterns were recorded on a Rigaku R-AXIS RAPID X-ray diffractometer. The samples were prepared by casting a drop of the nanostructure suspension onto a glass coverslip. The dried samples were coated with gold prior to SEM imaging. Both structure optimization and property calculations were performed using the standard 6-31G* basis set and the Becke's three parameter gradient-corrected hybrid density function B3LYP method with the Gaussian 03 program [23, 24].

Preparation of N-HQ

The synthesis of N-HQ is shown in Scheme 1. p-Chloroaniline (1.33 g, 20.0 mmol) was dissolved in hydrochloric acid (20 mL, 0.5mol/l) at 0-5℃ in an ice bath, and sodium nitrite (1.5 g, 21.0 mmol) was then added to the solution. The reaction mixture was stirred for 25 min to obtain p-chloroaniline diazo salt solution. 8-HQ (2.9 g, 20.0 mmol) and glacial acetic acid (8.0 mL) were added to another beaker, and this solution was slowly added to the prepared p-chloroaniline diazo salt solution under stirring. The mixture was stirred for an additional 20 min, resulting a large amount of orange yellow solid precipitates. The crude product was repeatedly washed and dried with deionized water, and then recrystallized with anhydrous ethanol/chloroform (2: 1) to obtain an

orange-red solid (5.0g, 75%). Characterization data: ^{1}H NMR ($CDCl_3$, 300 MHz): δ 9.31 (d, 1H, J = 9.30 Hz), 8.90 (s, 1H), 8.09 (d, 1H, J = 8.08 Hz), 7.86 (d, 2H, J =7.87 Hz), 7.66 (d, 2H, J =7.87 Hz), 7.30 (m, 2H). ^{13}C NMR ($CDCl_3$，75 MHz): δ 148.44, 146.17, 145.51, 140.81, 138.72, 128.42, 123.21, 115.75, 109.82. IR (KBr), ν, cm^{-1}: 3290, 1571, 1509, 1474, 1442. ESI-MS, m/z: 283.05 $[M+H]^+$. Elemental analysis: Calculated for $C_{15}H_{10}ClN_3O$, C 63.50, H 3.55, Cl 12.50, N 14.81, O 5.64%; found C 63.37, H 3.42, Cl 12.29, N 14.81, O 5.91%.

Preparation of C-HQ

The synthesis of C-HQ is also shown in Scheme 1. 5-Formyl-8-hydroxyquinoline (compound **2**) was synthesized according to the literature procedure [25]. Next, p-Chloroaniline (1.33 g, 20.0 mmol) and 5-formyl-8-hydroxyquinoline (3.5 g, 20.0 mmol) were dissolved in anhydrous ethanol (100 mL). Then, ice acetic acid (0.1 g) was added, and the mixture was stirred and heated refluxed for 7 h. After cooling, the crude product was filtered. The crude product was repeatedly washed and dried with deionized water, and then recrystallized in anhydrous ethanol/chloroform (1: 1) to obtain a yellowish solid (4.6 g, 71%). Characterization data: ^{1}H NMR ($CDCl_3$, 300 MHz): δ 9.92 (d, 1H, J = 9.91 Hz), 8.86 (d, 1H, J = 8.85 Hz), 8.72 (s, 1H), 7.88 (d, 1H, J =7.87 Hz), 7.65 (m, 1H), 7.52 (d, 2H, J =7.54 Hz), 7.25 (d, 1H, J =7.24 Hz), 7.14 (d, 1H, J =7.13 Hz). ^{13}C NMR ($CDCl_3$, 75 MHz): δ 160.86, 155.33, 151.50, 148.24, 138.22, 135.48, 135.22, 132.32, 126.85, 122.55, 119.01, 109.32. IR (KBr), ν, cm^{-1}: 3294, 1570, 1511, 1484, 1288. ESI-MS, m/z: 281.05 $[M+H]^+$. Elemental analysis: Calculated for $C_{16}H_{10}ClN_2O$, C 68.21, H 3.58, Cl 12.58, N 9.94, O 5.68%; found C 68.27, H 3.53, Cl 12.45, N 9.83, O 5.85%.

Results and Discussion

Synthesis and characterization

N-HQ and C-HQ were fully characterized by ^{1}H NMR, ^{13}C NMR, FT-IR and HR-MS. In the ^{1}HNMR of N-HQ and C-HQ, no signal of -OH was observed. However, the infrared spectra show peaks at 3290 cm^{-1} (N-HQ) and 3294 cm^{-1} (C-HQ), which confirm the presence of -OH groups. Both N-HQ and C-HQ are soluble in common organic solvents, such as dichloromethane, chloroform, tetrahydrofuran, and N, N-dimethylformamide.

Optical properties

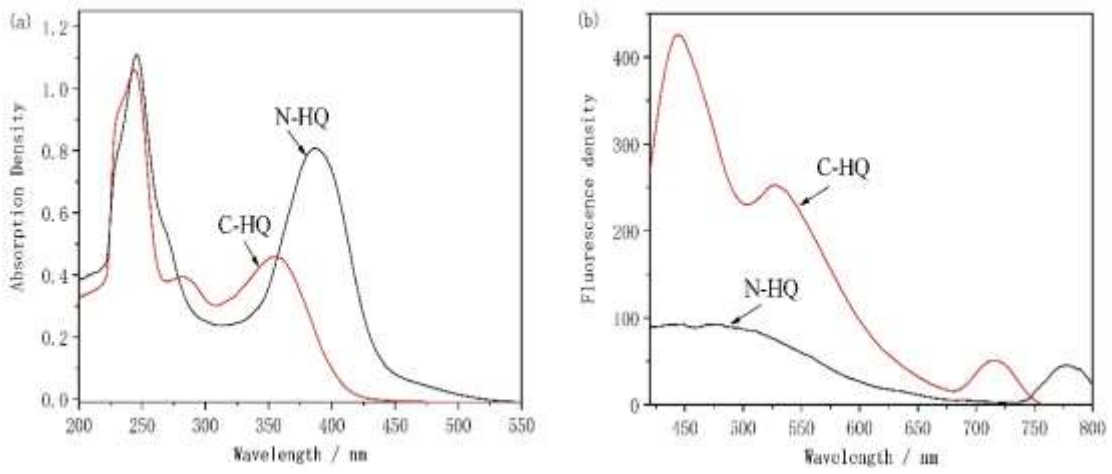

Fig. 1: UV-vis absorption (a) and emission (b) spectra of N-HQ and C-HQ in DCM solution (1×10^{-5} mol·L^{-1}).

Fig 1a shows the UV-vis absorption spectra of N-HQ and C-HQ in dichloromethane (10 μM). N-HQ and C-HQ exhibit strong absorption in the 200 nm to 550 nm range, with maximum absorption wavelengths of 246 nm (N-HQ) and 244 nm (C-HQ). After the chlorobenzene group was connected to 8-HQ by an N=N bond and a C=N bond, although the connection mode was similar, their spectral morphology and maximum absorption wavelengths were significantly different. N-HQ and C-HQ have strong absorption peaks at 386 nm and 356 nm, respectively. N-HQ has a redshift of 30 nm compared with C-HQ, because both the N=N bond and the C=N bond can connect the aromatic ring system to form a large conjugated system, and the π electron has a large delocalization range, allowing the entire molecule to absorb visible light and exhibit color. The N=N bond has more unbonded N electrons than the C=N bond, which reduces the energy level difference of the n-π* transition of N-HQ, results in a redshift in the absorption peak, and increases the absorption intensity. Fig 1b shows the fluorescence emission spectra of N-HQ and C-HQ in dichloromethane. N-HQ exhibits weak fluorescence, while C-HQ exhibits stronger fluorescence with an emission wavelength of 444 nm.

Electrochemical and thermal properties

As shown in Fig 2a, the electrochemical properties of N-HQ and C-HQ were measured by cyclic voltammetry. C-HQ showed a set of reversible reduction peaks in dichloromethane solution, while N-HQ showed a set of irreversible reduction peaks, indicating that the REDOX reaction of C-HQ is reversible, while that of N-HQ is irreversible, highlighting the distinct electrochemical behavior of the two compounds. N-HQ can gain one more electron than C-HQ. C-HQ has three oxidation peaks, while N-HQ has only one, indicating that C-HQ is more likely to undergo oxidation and less likely to undergo reduction, possibly because the carbon in the C=N bond is less electronegative than the nitrogen in the N=N bond. Using ferrocene as the standard, the first reduction peaks of N-HQ and C-HQ are -1.05V and -1.04V, respectively. Using the formula $E_{LUMO} = -$ [Ered (onset) + 4.8] eV [26], N-HQ and C-HQ have LUMO levels of -3.75 eV and -3.76 eV, respectively. The first oxidation peaks of N-HQ and C-HQ are 0.66V and 0.14 V, respectively. Using the formula $E_{HOMO} = -$ [Eox (onset) + 4.8] eV, the HOMO levels of N-HQ and C-HQ are −5.46 eV and −4.94 eV, respectively. According to the formula Egap = Ered1−Eox1, the E^{opt}gap of N-HQ and C-HQ is 1.71 eV and 1.18 eV, respectively. Thermogravimetric analysis (TGA) revealed that the two compounds only began to decompose after 240°C, with C-HQ being more stable than N-HQ (Fig 2b). The decomposition of N-HQ occurs at 240°C with a weight loss of 35%, which is close to the loss of chlorobenzene. The decomposition of N-HQ occurs at 250°C with a weight loss of 46%, which is likely due to the decomposition of chloroaniline.

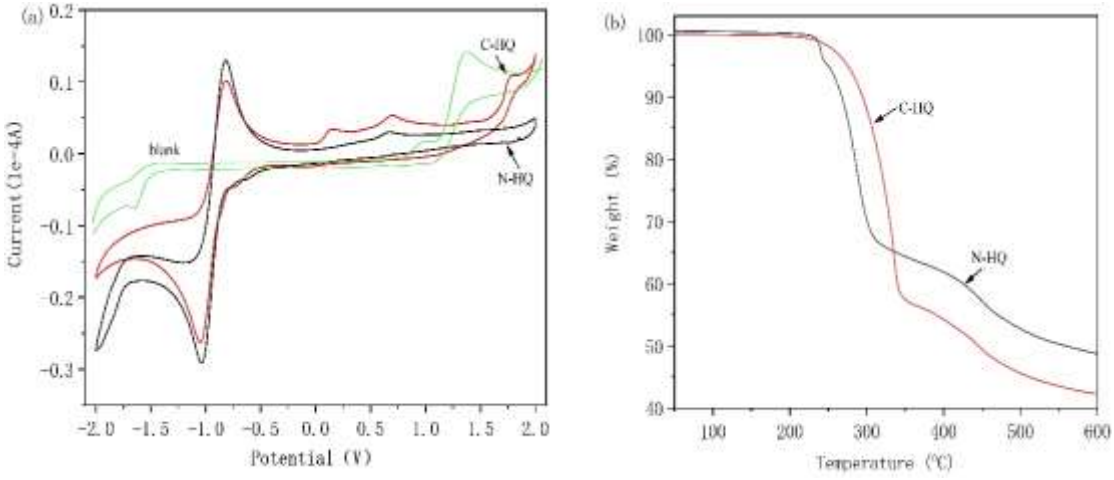

Fig. 2: The cyclic voltammogram (a) and TGA analysis (b) of N-HQ and C-HQ.

Quantum chemistry computation

In order to further study the molecular structure and properties of N-HQ and C-HQ, we used density functional DFT, B3LYP method and standard 6-31G* polarization group to optimize the configuration and properties of the two compounds. Their molecular configurations and the LUMO-HOMO of the front orbital are shown in Fig 3. Their optimized geometry showed that the spatial angles between the quinoline group and chlorobenzene were 0.002° and 42°, respectively. The planarity of the molecules varies greatly depending on their connectivity. According to theoretical calculations, the LUMO and HOMO of N-HQ and C-HQ are distributed in large conjugated systems, including quinoline groups, N=N bonds and C=N bonds with chlorobenzene. The HOMO/LUMO energy levels of N-HQ and C-HQ were estimated to be -0.26/-0.047 eV and -0.26/-0.064 eV, respectively. The results differ from those obtained through electrochemical properties. Because theoretical calculation provides energy levels in the ideal vacuum state, whereas the electrochemical methods provide energy level in the solution state. This disparity underscores the significant influence of solvent on the HOMO-LUMO level of N-HQ and C-HQ.

Aggregation behaviors of N-HQ and C-HQ

Self-assembly of N-HQ and C-HQ to nanostructure was achieved by a slow solvent-evaporation process. Approximately 10 mg of N-HQ and C-HQ were dissolved in 50 mL of dichloromethane. After allowing the solvent evaporate at room temperature over 10 days, nanostructures were obtained. Fig. 4a shows the SEM image of N-HQ nanosheets, exhibiting uniform width and thickness. The nanosheets have an average width ranging between 5-15 μm and lengths of 50-100 μm. In contrast, the SEM image of the C-HQ (Fig. 4b) reveals molecules assembled into 1D nanosheet with an average width of 1.0 μm and lengths extending tens of micrometers. Due to its approximate planar configuration, N-HQ molecules maintain a face-to-face π–π packing arrangement, resulting in highly ordered molecule packing in the solid state. conversely, adjacent C-HQ molecules exhibit a transverse offset, influencing their packing structure accordingly.

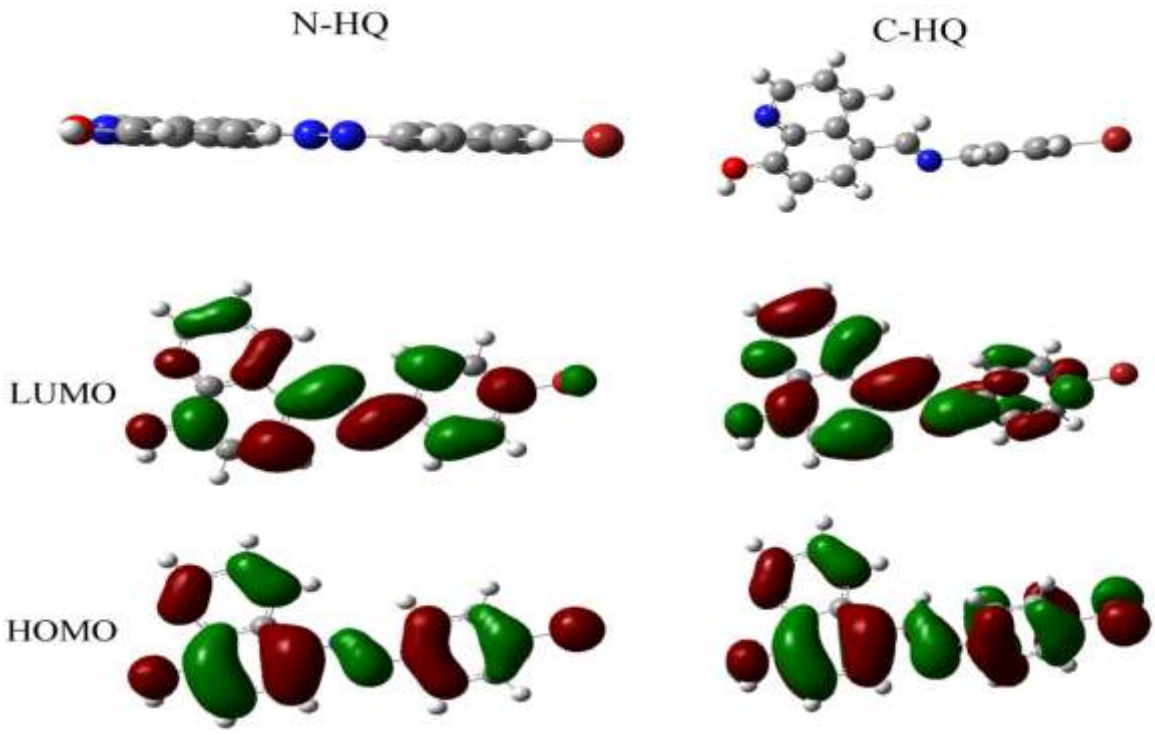

Fig. 3 Molecule structure (upper graphs) and computed frontier orbitals (lower graphs) of N-HQ and C-HQ.

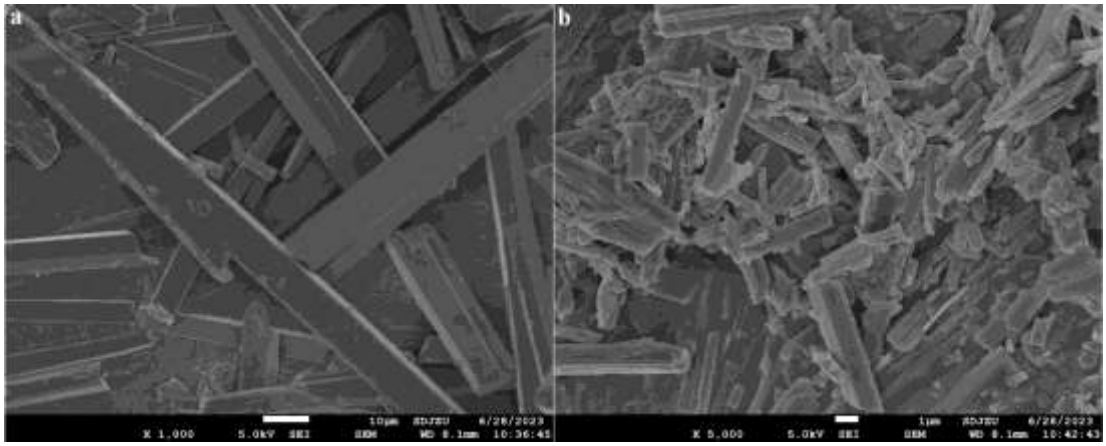

Fig. 4: Self-assembled structures of N-HQ **(a)** and C-HQ **(b)** deposited on a glass slide.

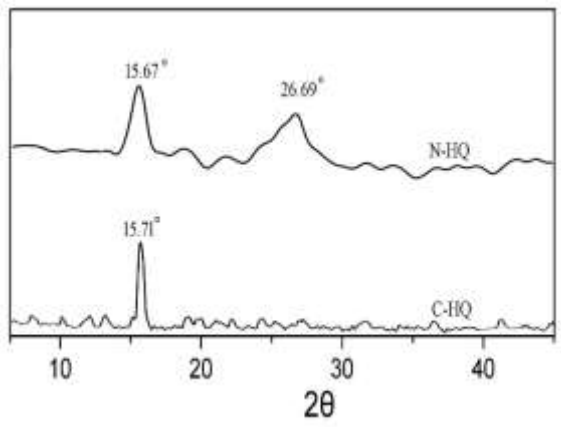

Fig. 5: X-ray diffraction analysis of the N-HQ and C-HQ.

The internal structures of the self-assembled N-HQ and C-HQ were further investigated using X-ray diffraction (XRD) (Fig. 5). The diffraction patterns were complex and could not be fully assigned. In the X-ray diffraction pattern of N-HQ, a peak at 2θ= 26.69° (3.2 Å) was identified, attributed to the π-π stacking of adjacent N-HQ molecules. In comparison, the diffraction peak intensity of C-HQ was notably diminished, indicating weaker π-π interactions in C-HQ. Additionally, a diffraction peak at 2θ = 15.67° (5.63 Å) observed in the XRD of N-HQ, shifted slightly to 15.71° (5.61 Å) in C-HQ, suggesting a crystalline α-form structure.

Application of fluorine sensing

Among various anions, fluoride ion (F^-) has garnered significant attention due to its established roles in dental care and clinical treatment of osteoporosis. The sensing capability of C-HQ for F^- was investigated using emission spectroscopy. A standard solution of tetrabutylammonium salt was added to a CH_2Cl_2 solution of C-HQ. Upon excitation at 356 nm, C-HQ exhibited maximum fluorescence emission at 444 nm. As the concentration of F^- increased from 0 to 1×10^{-5} M, the fluorescence intensity of C-HQ gradually decreased (Fig. 6a). To assess the selectivity of C-HQ for F^-, competitive experiments were conducted with 5.0 equiv. of F^- and other anions (Cl^-, Br^-, I^-, ClO_4^-, SO_4^{2-}, $H_2PO_4^-$, and AcO^-). The fluorescence spectra of C-HQ with F^- were remained unaffected even in the presence of all anions simultaneously (Fig. 6b). The results indicate that C-HQ has high sensitivity and selectivity for F^-.

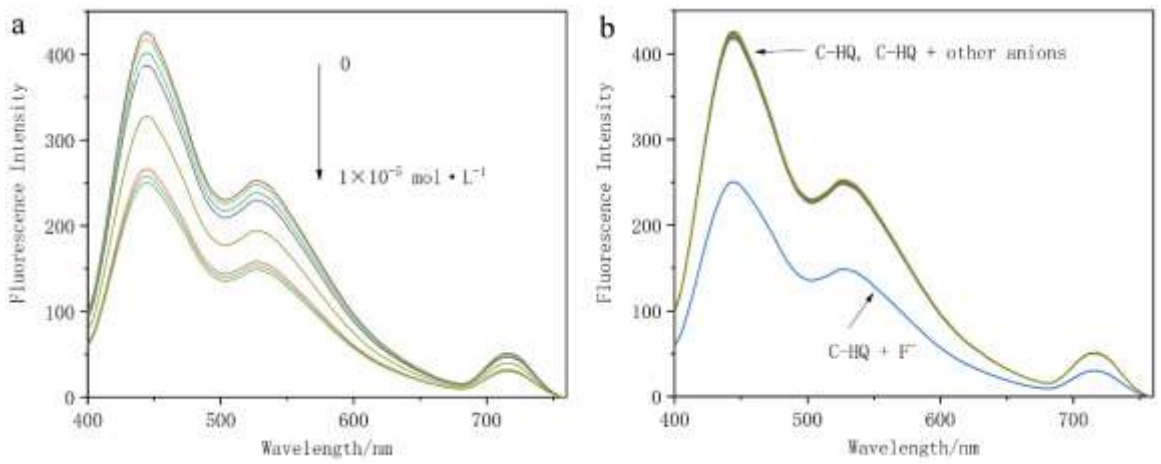

Fig. 6: (a) Fluorescence spectra changes of C-HQ (10^{-5} M) in CH_2Cl_2 solution in the presence of F^- ions only (0-1× 10^{-5} M). (b) Fluorescence spectra of C-HQ (10^{-5} M) in CH_2Cl_2 solution in the presence of various anions (5.0 equiv.).

Conclusions

N-HQ and C-HQ were synthesized by attaching a chlorobenzene group to 8-HQ via N=N and C=N bonds, respectively. Both compounds were extensively characterized. Due to the distinct bonding modes of chlorobenzene groups, their photochemical properties, electrochemical properties, spatial configurations, HOMO-LUMO energy levels, and aggregation behaviors exhibit significant differences. This demonstrates that even subtle variations in substituent group bonding can profoundly influence the physical and chemical properties of 8-HQ derivatives. These findings are crucial for guiding the development of photoelectric materials using 8-HQ derivatives as raw materials.

References

1. B. Elyor, V. Chandrabhan, B. Khasan, M. A. Quraishi, K. Abduvali, A. Khamdam, U. Nurbek, B. Bakhtiyor, 8–Hydroxyquinoline is key to the development of corrosion inhibitors: An advanced review, *Inorg. Chem. Commun.*, **144**, 109839 (2022).
2. M. Galai, M. Rbaa, M. Ouakki, L. Guo, K. Dahmani, K. Nouneh, S. Briche, B. Lakhrissi, N. Dkhireche, M. Touhami, Effect of alkyl group position on adsorption behavior and corrosion inhibition of new naphthol based on 8-hydroxyquinoline: Electrochemical, surface, quantum calculations and dynamic simulations, *J. Mol. Liq.*, **335**, 116552 (2021).
3. V. Oliveri, G. Vecchio, 8-Hydroxyquinolines in medicinal chemistry: A structural perspective, *Eur. J. Med. Chem.*, **120**, 252 (2016).
4. J. Kos, C. F. Ku, I. Kapustikova, M. Oravec, H. J. Zhang, J. Jampilek, 8-Hydroxyquinoline-2-carboxanilides as antiviral agents against avian influenza virus, *Chem. Select.*, **4**, 4582 (2019).
5. H. Xu, W. Chen, P. Zhan, X. Liu, 8-Hydroxyquinoline: A privileged structure with a broad-ranging pharmacological potential, *Med. Chem. Comm.*, **6**, 61 (2015).
6. Z. M. Alamshany, A. A. Ganash, Synthesis, characterization, and anti-corrosion properties of an 8-hydroxyquinoline derivative. *Heliyon*, **5**, 2895 (2019).
7. S. Indira, G. Vinoth, M. Bharathi, K. S. Bharathi, Synthesis, spectral, electrochemical, in-vitro antimicrobial and antioxidant activities of bisphenolic mannich base and 8-hydroxyquinoline based mixed ligands and their transition metal complexes, *J. Mol. Struct.*, **1198**, 126886 (2019).
8. I. Cacciatore, E. Fornasari, L. Baldassarre, C. Cornacchia, S. Fulle, E. S. Filippo, T. Pietrangelo, F. Pinnen, A Potent (R)-alpha-bis-lipoyl derivative containing 8-hydroxyquinoline scaffold: synthesis and biological evaluation of its neuroprotective capabilities in SH-SY5Y human neuroblastoma cells, *Pharmaceuticals*, **6**, 54 (2013).
9. S. H. Chan, C. H. Chui, S. W. Chan, S. H. Kok, D. Chan, M. Y. Tsoi, P. H. Leung, A. K. Lam, A. S. Chan, K. H. Lam, J. C. Tang, Synthesis of 8-

hydroxyquinoline derivatives as novel antitumor agents, *ACS. Med. Chem. Lett.*, **4**, 170 (2012).
10. A. Chaouiki, M. Chafiq, M. Rbaa, H. Lgaz, R. Salghi, B. Lakhrissi, I. H. Ali, S. Masroor, Y. Cho, New 8-hydroxyquinoline-bearing quinoxaline derivatives as effective corrosion inhibitors for mild steel in HCl: Electrochemical and computational investigations, *Coatings.*, **10**, 811 (2020).
11. C. Verma, M. A. Quraishi, E. E. Ebenso, Quinoline and its derivatives as corrosion inhibitors: A review, *Surf. Interfaces*, **21**, 100634 (2020).
12. D. J. Richard, R. Lena, T. Bannister, N. Blake, W. E. Pierceall, N. E. Carlson, C. E. Keller, M. Koenig, Y. He, D. Minond, J. Mishra, M. Cameron, T. Spicer, P. Hodder, M. H. Cardone, Hydroxyquinoline-derived compounds and analoguing of selective Mcl-1 inhibitors using a functional biomarker, *Bioorg. Med. Chem.*, **21**, 6642 (2013).
13. K. Hanaya, M. Suetsugu, S. Saijo, I. Yamato, S. Aoki, Potent inhibition of dinuclear zinc(II) peptidase, an aminopeptidase from Aeromonas proteolytica, by 8-quinolinol derivatives: inhibitor design based on Zn^{2+} fluorophores, kinetic, and X-ray crystallographic study, *J. Biol. Inorg. Chem.*, **17**, 517 (2012).
14. A. F. Eweas, G. Allam, A. S. Abuelsaad, A. H. Alghamdi, I. A. Maghrabi, Design, synthesis, anti-schistosomal activity and molecular docking of novel 8-hydroxyquinoline-5-sufonyl 1,4-diazepine derivatives, *Bioorg. Chem.*, **46**, 17 (2013).
15. S. Ariyasu, A. Sawa, A. Morita, K. Hanaya, M. Hoshi, I. Takahashi, B. Wang, S. Aoki, Design and synthesis of 8-hydroxyquinoline-based radioprotective agents, *Bioorg. Med. Chem.*, **22**, 3891 (2014).
16. S. N. Busafi, F. E. O. Suliman, Z. R. Alawi, 8-Hydroxyquinoline and its derivatives: Synthesis and applications, *Res. Rev. J. Chem.*, **3**, 1 (2014).
17. V. Oliveri, G. Vecchio, 8-Hydroxyquinolines in medicinal chemistry: A structural perspective, *Eur. J. Med. Chem.*, **120**, 252 (2016).
18. J. A. Love, I. Nago, Y. Huang, M. Kuik, V. Gupta, C. J. Takacs, J. E. Coughlin, L. Qi, S. P. Thomas, E. J. Kramer, A. J. Heeger, T. Q. Nguyen, G. C. Bazan, Silaindacenodithiophene-based molecular donor: morphological features and use in the fabrication of compositionally tolerant, high-efficiency bulk heterojunction solar cells, *J. Am. Chem. Soc.*, **136**, 3597 (2014).
19. A. J. Jimenez, M. J. Lin, C. Burschka, J. Becker, V. Stetteles, B. Engels, F. Würthner, Structure–property relationships for 1,7-diphenoxy-perylene bisimides in solution and in the solid state, *Chem. Sci.*, **5**, 608 (2014).
20. H. A. Saadeh, K. A. Sweidan, M. S. Mubarak, Recent advances in the synthesis and biological activity of 8-hydroxyquinolines, *Molecules*, **25**, 4321 (2020).
21. E. Ahmetali, B. Yıldız, E. E. Ahi, M. Durmuş, M. K. Şener, Synthesis, photophysical and photochemical properties of unsymmetrical zinc(II) phthalocyanines bearing 8-hydroxyquinoline unit, *Polyhedron*, **226**, 116111 (2022).
22. J. Wu, L. Lu, P. Mei, Design, characteristics, and theoretical analyses of 8-hydroxyquinoline derivatives with different heteroatoms as effective corrosion inhibitors, *Mater. Chem. Phys*, **304**, 127929 (2023).
23. A. D. Becke, Density-functional thermochemistry. III. The role of exact exchange, *J. Chem. Phys.*, **98**, 5648 (1993).
24. A. D. Becke, Density-functional exchange-energy approximation with correct asymptotic behavior, *Phys. Rev. A.*, **38**, 3098 (1998).
25. S. T. Tan, J. P. Zhou, B. Zhao, J. H. Peng, Preparation and photoluminescent property of polymeric dis(8-hydroxyquinoline Schiff base) zinc complexes, *Chin. J. Lumin.*, **24**, 51 (2003).
26. Y. Jiang, L. Lu, M. Yang, C. Zhan, Z. Xie, F. Verpoort, S. Xiao, Taking the place of perylene diimide: perylene tetracarboxylic tetraester as a building block for polymeric acceptors to achieve higher open circuit voltage in all-polymer bulk heterojunction solar cells, *Polym. Chem.*, **4**, 5612 (2013).